COMMSCOPE®

An introduction to LTE
Smart base station antennas

Mobility Network Engineering
February 2017

Dr. Mohamed Nadder Hamdy

Table of Contents

List of figures

Introduction

We are in the midst of yet another technology upheaval in which everyday objects—from clothing to cars—are being converted into smart devices. Smart phones and smart TVs give rise to smart homes and intelligent buildings, which evolve and expand into smart grids, smart cities and smart governments. It's no surprise, then, that the traditional base station antenna is following a similar path.

This paper provides a brief overview of the evolution of smart antennas and their sometimes-confusing relationship to active antennas, beamforming, precoding and MIMO transmission modes.

Unlike traditional antennas that could transmit and receive only using a fixed radiation pattern regardless of the environment, smart antennas are adaptive beamformers. They can dynamically adjust the main beam and nulls directions in their patterns according to channel conditions and the locations of connected users.

For example, using digital signal processing (DSP) techniques, smart antennas are able to estimate the direction of arrival (DoA) for a connected device and shape the radiating patterns accordingly. To better understand how these techniques work, we need to take a closer look at some of the technologies that make them possible:

- Principles of phased antenna arrays
- Beam steering using switched beam antennas
- Beamforming with adaptive array antennas
- Precoding and Eigen beamforming systems

Smart Antennas possess "Super Powers" to dynamically adjust their main beams and nulls directions

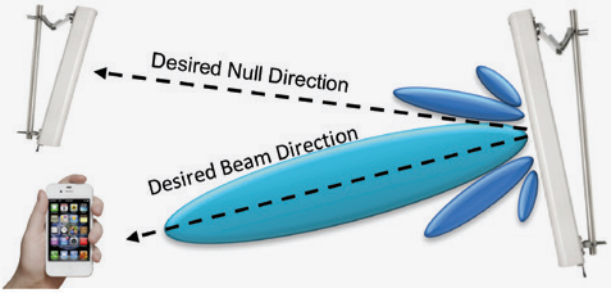

Figure 1, Beams and Nulls Steering

Phased array antennas

A phased array antenna applies phase control (or time delay) at each radiating element, so its beam can be scanned to different angles in space. Here is how it's constructed.

Antenna array patterns

A typical base station panel antenna consists of a number of radiating antenna elements (AE). Some examples can be seen in Figure 2.

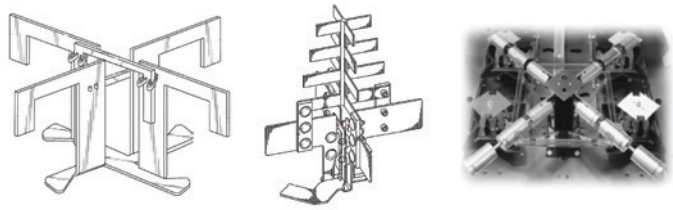

Figure 2, Andrew patented antenna elements examples

There are different types of AEs, with wire and aperture elements being the most common. Examples of wire AEs include dipole and monopole elements, while aperture AEs include slot elements. Some designs incorporate combinations of both types and can also be built over printed circuit boards or micro strip patches. Every AE has a radiation pattern, usually referred to as an **element pattern,** whose characteristics are determined by the design of the element.

When multiple AEs are mounted in a line along a shared reflector, the result is a panel antenna with linear arrays (Figure 3).

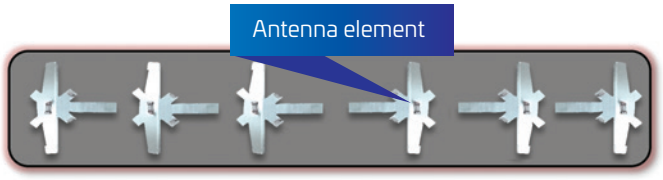

Figure 3, Base station panel antenna

While each AE in a linear array has its own radiation pattern, the RF effect of the entire array depends on the **spacing, phase shifts** and **amplitude variation** between its elements. Together, these three variables are used to describe the **array factor pattern.** By combining the array factor pattern and the element pattern, we can determine the overall far-field radiation pattern of the panel antenna.

The RF signal phases and amplitudes feeding the AEs can be controlled in order to shape the array factor pattern. This eventually directs and shapes the final beam.

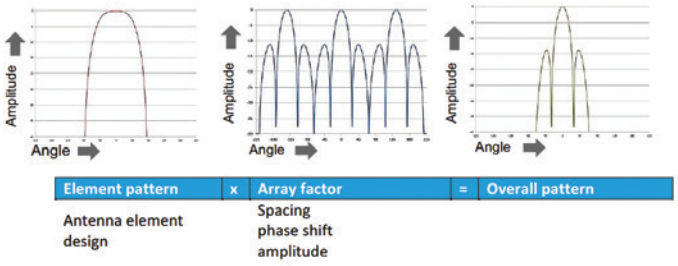

Figure 4, Array factor

Electrical downtilt

Electrical downtilting—a primitive beamforming technique for vertical patterns—has now become a standard feature in almost all base station antennas (BSAs). As with the phased array antenna, electrical downtilt works by adjusting the phase shifters, which alters the panel's array factor. The polar plot in Figure 5 illustrates the effect phase shifting has on the direction of the main lobe.

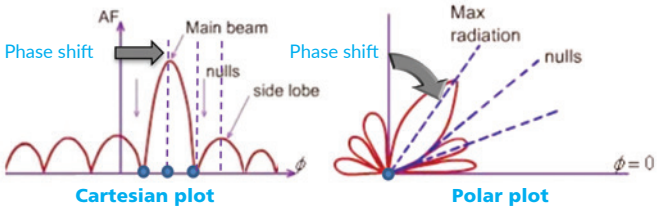

Figure 5, Antenna elements phase shifts

The antenna's "electrical" downtilt is actually accomplished mechanically, as the phase shifters are adjusted either manually on the antenna itself or remotely using a controlled stepper dc motor. Figure 6 shows a dual polarized antenna with electrical tilt. The phase shifters can be clearly seen connected to the Antenna Elements' feeding network.

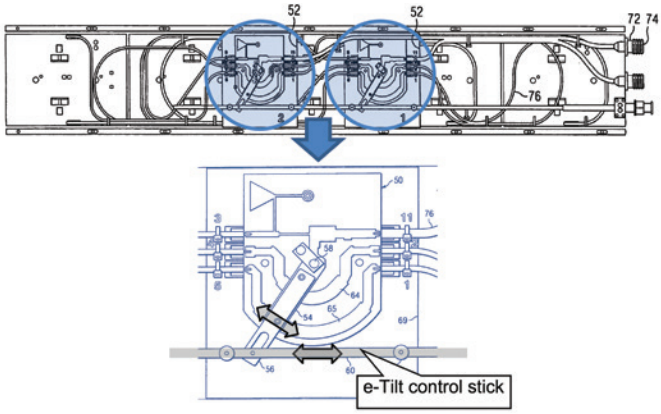

Figure 6, Andrew Patent U.S. 6924776 B2

Switched beam antennas

The switched beam antenna represents the next step in the evolution toward the smart antenna. It consists mainly of an antenna array and simple beamforming network capable of generating a number of discrete predefined fixed beam directions. The system dynamically selects the best beam for spatial selectivity based on channel conditions. Two of the more popular switched beam antenna designs include the Butler matrix and Luneburg lens.

Butler matrix

The **Butler matrix**, first described by Jesse Butler and Ralph Lowe in 1961, uses hybrid combiners and phase shifters.

As shown in Figure 7, all four input ports (1R, 2L, 2R and 1L) are mapped to all four AEs (#1, #2, #3, #4) but with different phase shift combinations. As a result, each input port is able to generate a different beam direction.

Moreover, when an input signal is switched across all input ports—such that one port is connected at a time—and the proper switch position is selected, the beam can be electrically steered toward specific traffic areas.

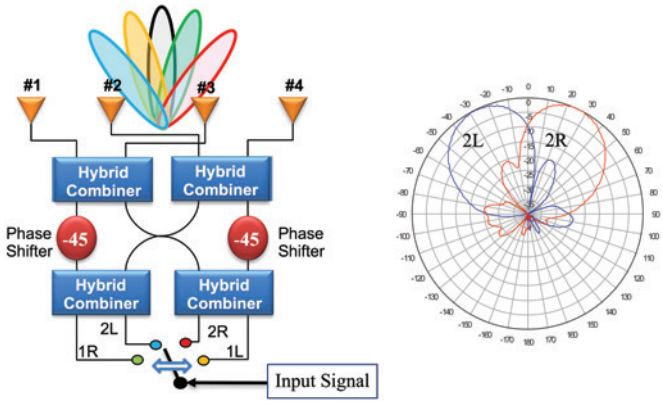

Figure 7: RF path and radiation pattern of a four-port Butler matrix antenna

Luneburg lens

The Luneburg lens was first proposed by Dartmouth College professor Rudolf Karl Lüneburg in 1944. Luneburg lenses are typically composed of layered structures of discrete concentric shells that form a stepped refractive index profile. The different refractive indices decrease radially from the center to the outer surface.

The Luneburg lens can be utilized for electromagnetic radiations, ranging from visible light to radio waves. The lens's variable refractive indices align and direct the radiated waves from its surface in one direction, as shown in Figure 8. Similar to the Butler matrix, the direction of the antenna beam can be scanned by moving the radiating element along the lens's circumference.

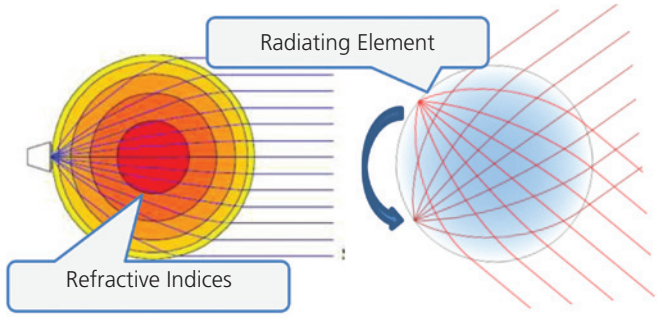

Figure 8, Luneburg lens construction

Adaptive array antennas (AAA)

Planar arrays

We have seen how beamforming techniques rely on the alteration of the RF signal phases and amplitudes that are fed across the internal antenna radiating elements. For linear array antennas, vertical beam steering (e-tilting) is a direct application of this concept. However, to enable horizontal and vertical beam steering, a two-dimensional rectangular array is needed. This is known as a planar array, a key component of today's adaptive array antennas (AAA).

Adaptive array antennas consist of columns of a planar array that work together to form a steerable beam that is shaped for improved side lobes[i]. Adaptive beamforming uses digital signal processing technology to identify the RF signal's direction of arrival (DoA) to a User Equipment (UE)—and generate a directional beam towards it[ii].

CommScope TTTT series

For many, the common belief has been that any successful adaptive antenna array must involve active antennas or antennas with integrated radios. However, it is actually possible to achieve horizontal electrical beam steering over regular antennas with the support of external base station radios[iii]. The CommScope TTTT antenna series is a good example of this capability.

Horizontal beam steering is realizable with mutli-column antennas and external radios

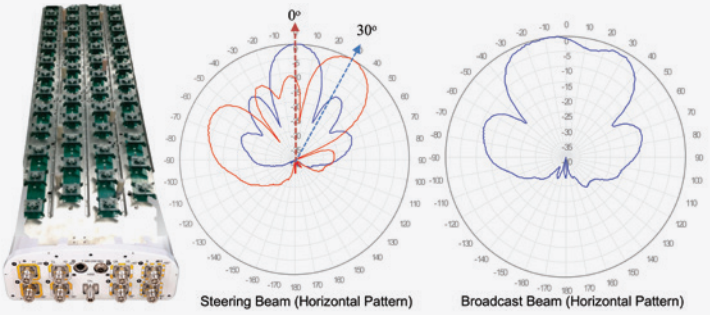

Figure 9, CommScope TTTT65AP-1XR antenna

There are currently two TTTT series models in CommScope's portfolio.

Model Number	Horizontal Beamwidth	Gain (dBi)	Vertical Beamwidth	Frequency (MHz) / No. of PortS
TTT65AP-1XR	65°	17.8	4.8°	2490-2690 / 8
TTTT90AP-1XR	90°	17.2	4.7°	2490-2690 / 8

Column pattern and mutual coupling

It should be noted that the horizontal beamwidth (H-BW) listed in TTTT series datasheets is not reflective of the entire panel. Instead, it shows the pattern shape for one of the antenna's four identical columns. Such column pattern shape is dependent on a number of physical features. These include radiating elements design, reflector widths and, most importantly, **intercolumn spacing**.

Because an array's behavior is dominated by the mutual coupling between its various elements, the elements generally behave very differently in an array than when isolated[iv]. For example, the H-BW listed on the datasheet is inversely affected by column spacing: a 65-degree H-BW typically requires 0.65 λ spacing between columns, whereas a 90-degree H-BW will use 0.5 λ spacing. Figure 10 shows this effect for a 7x9 element dipole array (λ/2 dipoles, λ/4 above ground.) Element spacings are denoted as D_x and D_y.

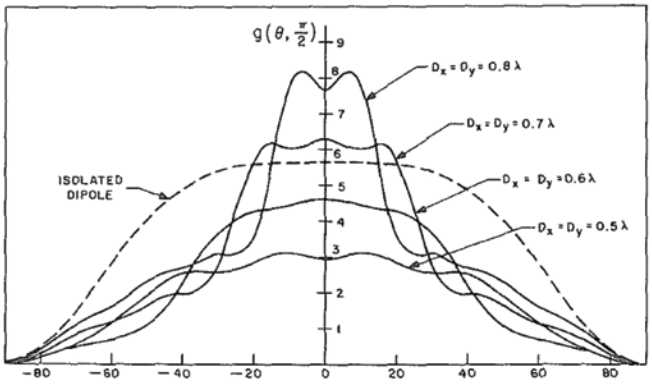

Figure 10, Element spacing and H-BW[v]

Scanning angle limitations

A linear array with its peak at Θ_o can also have other peak values, depending on its spacing d_x. These additional unwanted peaks are called **"grating lobes."** To avoid these lobes, it is important to observe the relationship between the column pattern horizontal half-power beamwidth (H-HPBW) and the maximum scanning angle. For element spacing d_x ($0.5\ \lambda < d_x < \lambda$), the array factor will have only one single major lobe, and grating-lobe maxima will not occur for $-90° < \Theta_o < +90°$ as long as[vi]

$$|\sin\theta_0| > \frac{1}{S} - 1 < \text{where } \mathbf{S} = d_x/\lambda$$

Plotting this relationship for different column spacings, as in Figure 11, it is clear the condition is always true for **0.5** λ (S=0.5) column spacing, which leads to the **±90-degree** scanning angle range. For max scanning angles of **±32**, ±45 and ±60 degrees, the spacing is **0.65** λ**,** 0.59 λ and 0.53 λ, respectively.

Therefore, **0.5** λ intercolumn spacing corresponds to the **90-degree** column H-BW with **±90-degree** antenna scanning angle range. Similarly **0.65** λ corresponds to **65-degree** column H-BW with **±32-degree** antenna scanning angle range.

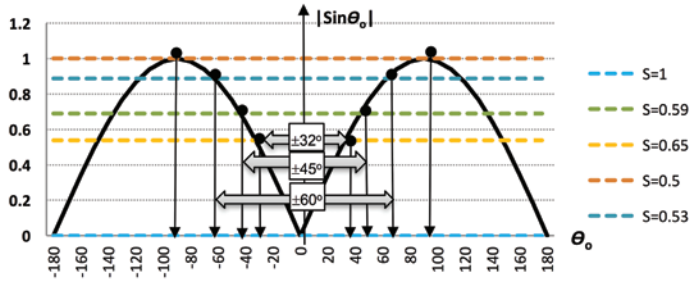

Figure 11, Max scan angle versus column spacing

Radiating patterns

An adaptive array beamforming antenna has three main radiating pattern types:

I. Single column pattern

This pattern type, described in datasheets, uses unweighted inputs and is typically used for uplink channels.

II. Broadcast pattern

This **wider, nonsteerable beam** is intended to cover the entire cell area and is created by feeding the four columns with different amplitudes and phases. By reducing the amplitude, the broadcast pattern exhibits a gain reduction, also known as "weighting loss." The broadcast is usually used for downlink control channels.

III. Service beam pattern

When all columns are fed together with a uniform phase progression, the result is a **narrow beam that can be steered horizontally.** In a service beam pattern, the amplitudes might be unchanged—or tapered for side lobe suppression with added weighting losses. This type of radiating pattern is used mainly for downlink data traffic.

To generate these patterns, the RAN supplier radios must be able to apply different amplitude and phase shifts across the antenna ports. For example, for broadcast or service steering modes, the radios might apply the below-phase and amplitude difference across the antennas' four arrays (columns). See Table 1.

As shown in Figure 12, by using specific amplitude and phase settings, the TTTT65APand TTTT90AP are capable of generating 65-degree H-BW broadcast patterns. Ironically,the 90-degree model experiences less weighting loss for producing a 65-degreebroadcast pattern.

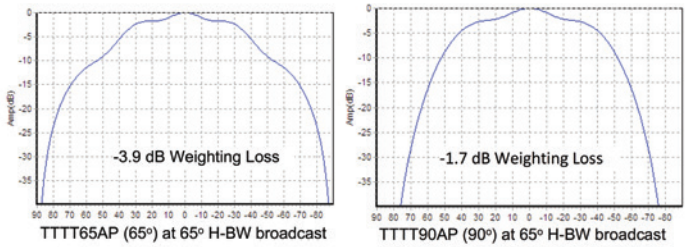

Figure 12, Broadcast beams patterns

Beam mode		Column 1	Column 2	Column 3	Column 4
65° Broadcast	Phase Φ	0	115	100	0
	Amplitude	0.81	1	0.73	0.6
90° Broadcast	Phase Φ	0	130	110	0
	Amplitude	0.79	1	0.75	0.6
Beam Steering @ 0°	Phase Φ	0	0	0	0
	Amplitude	1	1	1	1
Beam Steering @ 30°	Phase Φ	0	100	200	300
	Amplitude	1	1	1	1

Table 1, Beam steering settings

Calibration port

We have seen how the patterns of an AAA are dependent on its ports' phase and amplitude variations as listed in Table 1. These settings can be accurately applied from the radio's side, but this does not necessarily guarantee these exact values will arrive at the antenna ports. This is especially true given the variances in length of the connection jumpers being used. The calibration port, shown in Figure 13, is designed to compensate for any variance. In the example below, all sub-arrays are coupled to a single CAL port.

Figure 13, Calibration port on a CommScope antenna

Inside the CommScope TTTT antennas, a calibration board (Figure 14) built with Wilkinson Power dividers maintains a coupling level of -26 decibels toward the calibration port. The coupling level is a balance between power losses and meaningful calibration level for accurate calibration.

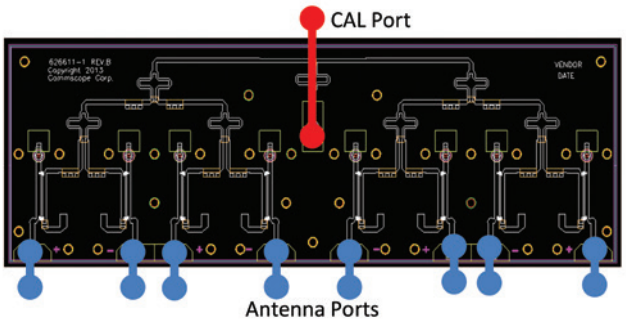

Figure 14, Calibration board

OEM radios must also be able to support the calibration functionality. This is done by designing the RRU with a dedicated CAL port (Figure 15) for connection to the corresponding CAL port on the antenna. This ensures accurate phase and amplitude settings, regardless of the feeders' lengths. The OEM radios shown also have eight antenna ports to support the four x-pol columns antennas.

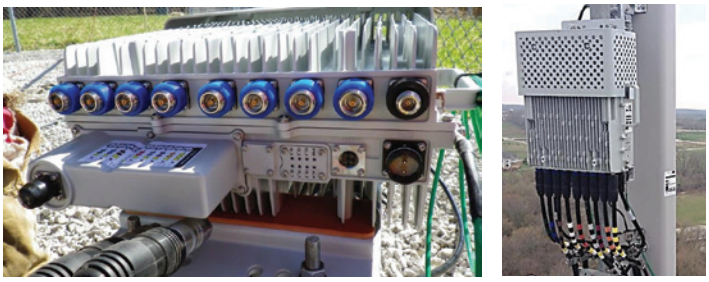

Figure 15, Sprint/SAMSUNG 8T8R implementation (U.S.)

Eigen beamforming (precoded MIMO)

In addition to the traditional beamforming capabilities of phased array antennas beamforming, LTE enables another beamforming effect resulting from channel precoding. The effect is commonly known as Eigen beamforming.

Figure 16 shows DL codeword processing by LTE physical layer.

Codeword: **a transport block after adding error protection as CRC, channel coding and rate matching. One or two code words, CW0 and CW1, may be used depending on the channel conditions and use case.** Layer: **represents the number of independent data streams that can be simultaneously transmitted. (e.g., MIMO streams).**

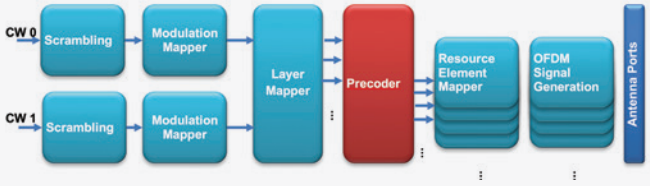

Figure 16, DL physical channel processing

Precoding

In a MIMO system, the final received signal is a result of destructive and constructive multipath reflections. When precoding is added, the transmitter—apprised of current channel conditions—can effectively combine the independent data streams prior to transmission in order to equalize signal reception across the multiple receive antenna[vii].In other words, the precoder reverses channel effects from the transmitter side.

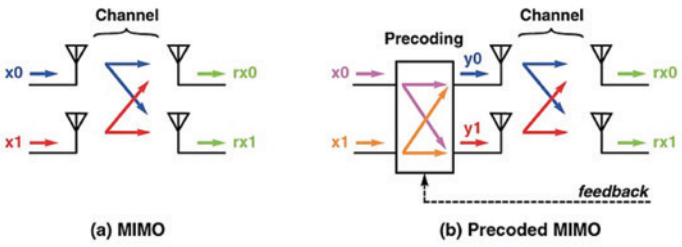

Figure 17, Precoded MIMO

MIMO precoding relies on the transmitter being able to acquire certain information from the user equipment (UE) reports regarding the channel. For instance, in the **open-loop** modes, the UE sends minimal information to the eNodeB. This includes:

- Rank indicator **(RI)**: Number of layers that can be supported under the current channel conditions and modulation scheme (e.g., single-layer SISO or two-layer 2x2 MIMO)
- Channel quality indicator **(CQI)**: Channel conditions status under the current transmission mode.

In **closed-loop modes,** the UE must also provide a precoding matrix indicator **(PMI)** in order to estimate the optimum precoding matrix for the current channel conditions.

LTE specifies a number of predefined codebooks, known at both transmitter and receiver sides as precoding matrices. Table 2 shows an example for two-antenna-port precoding codebooks, using single or dual layers.

Codebook index	Number of Layers υ	
	1	2
0	$\frac{1}{\sqrt{2}}\begin{bmatrix}1\\1\end{bmatrix}$	$\frac{1}{\sqrt{2}}\begin{bmatrix}1 & 0\\0 & 1\end{bmatrix}$
1	$\frac{1}{\sqrt{2}}\begin{bmatrix}1\\-1\end{bmatrix}$	$\frac{1}{2}\begin{bmatrix}1 & 1\\1 & -1\end{bmatrix}$
2	$\frac{1}{\sqrt{2}}\begin{bmatrix}1\\j\end{bmatrix}$	$\frac{1}{2}\begin{bmatrix}1 & 1\\j & -j\end{bmatrix}$
3	$\frac{1}{\sqrt{2}}\begin{bmatrix}1\\-j\end{bmatrix}$	

Table 2, Codebook for transmission on 2 antenna ports

Codebook **index 0,** the simplest precoding matrix, maps each layer to a single antenna, **without any coupling** to other antennas.

$$y^{(0)}(i) = \frac{1}{\sqrt{2}}\, x^{(0)}(i)$$

$$y^{(1)}(i) = \frac{1}{\sqrt{2}}\, x^{(i)}(i)$$

Codebook **index 1** provides a **linear combination** of the sums and differences of the two input layers, respectively.

$$y^{(0)}(i) = \frac{1}{2}\, x^{(0)}(i) + \frac{1}{2}\, x^{(i)}(i)$$

$$y^{(1)}(i) = \frac{1}{2}\, x^{(0)}(i) - \frac{1}{2}\, x^{(i)}(i)$$

As the precoding matrices apply **amplitude and/or phase shifts** to the input signal, the result is the **implicit Eigen beamforming** effect on the antennas' patterns, as shown in Figure 18.

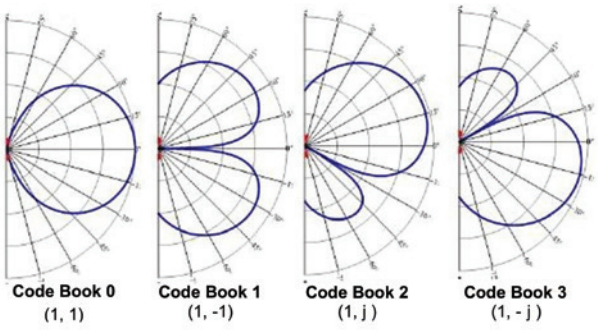

Figure 18, Two half-wavelength separated dipoles applying single-layer codebook [viii]

Antenna ports

In the LTE 3GPP standards, the term "antenna ports" often creates confusion. These ports, in fact, do not correspond to actual physical antennas, but are considered logical. As detailed in Table 3, LTE antenna ports have standard numbers that are mapped to the transmission of reference signals (RS) specific to the UE. These UE-specific RS signals are used for beamforming modes and must be supported by TDD UEs. FDD UEs may provide optional support.

Reference Signal	Antenna Ports
Cell specific RS	0
	0, 1
	0, 1, 2, 3
UE specific RS	5, 7, 8
	5, 7-14
MBSFN RS	4
MBSFN RS	6
CSI RS	15-22
Demodulation RS	107-110

Table 3, Reference signals mapping to antenna ports - 3GPP TS36.211 V12

Signals from multiple antenna ports can be transmitted on a single transmit antenna; conversely, a single antenna port can also be spread across multiple transmit antennas[ix]. In either case, the BTS is responsible for mapping logical antenna ports to physical ones.

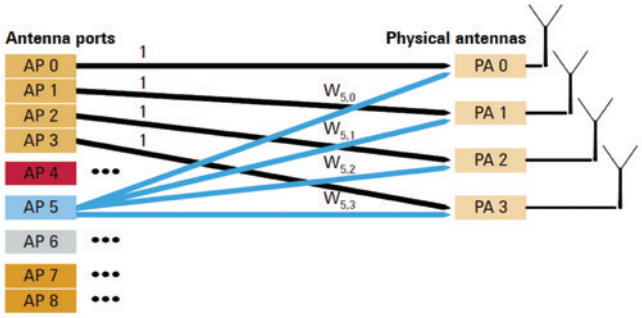

Figure 19, Mapping antenna ports to physical antennas.[x]

LTE MIMO schemes

LTE defines a number of its so-called transmission modes (TM). Depending on channel conditions, the TM can utilize **SISO** (single antenna), **MISO** (TX diversity), **MIMO** (spatial multiplexing) and **beamforming,** under closed- or open-loop transmission modes.

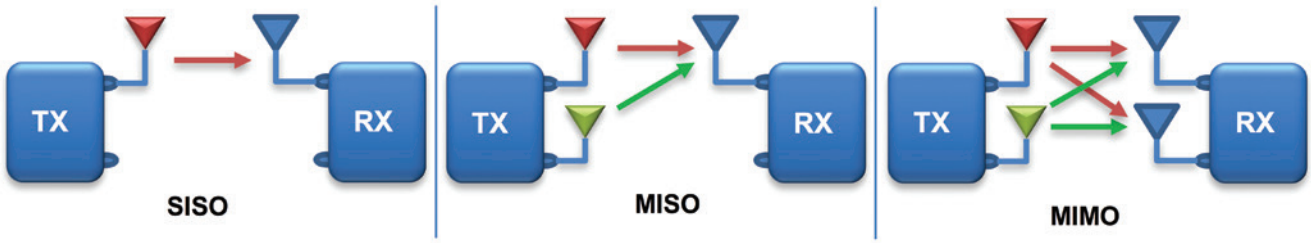

Figure 20, TX-RX modes

Table 4 shows an example of LTE transmission modes for PDCCH and PDSCH configured by C-RNTI (cell—radio network temporary identifier)[xi].

Trans. Mode	Mapping	Loop status	Transmission scheme of PDSCH corresponding to PDCCH	3GPP Release
TM1	SISO	Open	Single-antenna port, port 0	Rel.8
TM2	MISO	Open	Transmit diversity	Rel.8
TM3	MIMO	Open	Large delay Cyclic Delay Diversity (CDD)	Rel.8
TM4	MIMO	Closed	Closed-loop spatial multiplexing	Rel.8
TM5	MIMO	Closed	Multi-user MIMO	Rel.8
TM6	MIMO	Closed	Spatial multiplexing using single transmission layer	Rel.8
TM7	MIMO	Closed	Single-antenna port, port 5	Beamforming, Rel.8
TM8	MIMO		Dual layer transmission, port 7 and 8	Beamforming, Rel.9
TM9	MIMO		Up to 8 layer transmission, ports 7-14	Beamforming, Rel.10
TM10	MIMO		Up to 8 layer transmission, ports 7-14	Multiple Cell Beamforming, Rel.11

Table 4, LTE Transmission modes

As shown in Figure 21, the eNodeB applies different MIMO modes to different UEs, according to their signal quality, speed and other factors.

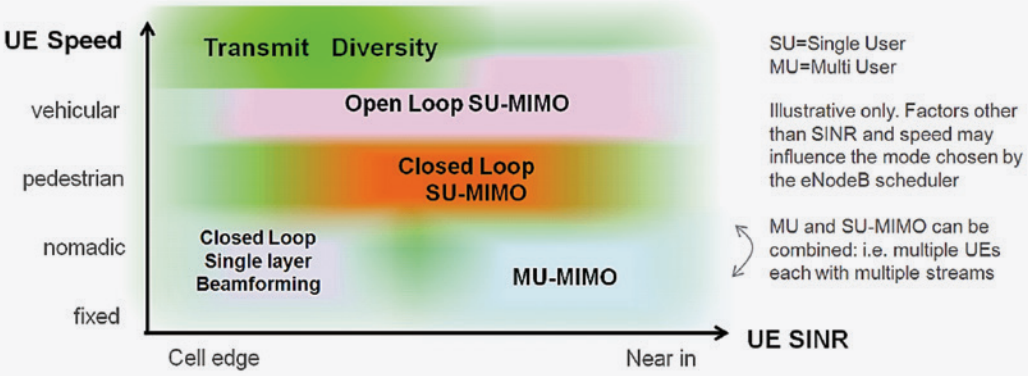

Figure 21, MIMO modes in LTE-advanced selected on the basis of UE SINR and speed[xii]

Practical implementation with the TTTT

Introduced earlier, CommScope's TTTT antenna series features eight external ports (excluding the CAL port) and four cross-polarized columns inside. This configuration supports a wide range of transmission modes and beamforming schemes.

Having eight external ports enables the antennas to be deployed in 8T8R TDD mode (eight branch transmit and eight branch receive).

As beamforming relies on columns with mutual coupling correlation, it requires columns of similar polarizations. Referring to Figure 22, the four cross-polarized columns can be thought of as four co-pol columns on ports 2, 4, 6 and 8 (red) and four cross-pol columns on ports 1, 3, 5 and 7 (blue). In other words, two beamforming antennas (BF1 and BF2) separated by polarization diversity.

Depending on the configuration of the radio, the TTTT can then support beamforming TM8, 9 and 10, listed in Table 4, with MIMO schemes ranging from 2x to 8x or multi-user MIMO. However, if configured as in Figure 22—two cross-polarized beamformers, each with four columns—we can see how the antenna can support 2x MIMO with beamforming. Table 5 provides a summary of useful tips in selecting antennas for beamforming and MIMO modes.
For more details on choosing the right antenna for LTE applications, see CommScope's white paper, *Base station antenna selection for LTE networks*[xiii].

The TTTT can support beamforming TM8, 9 and 10, with MIMO schemes ranging from 2x to 8x or multi-user MIMO.

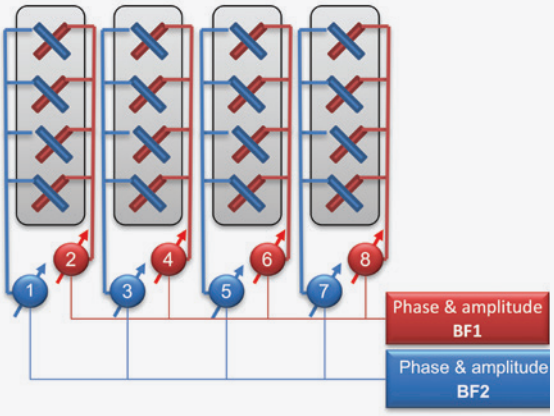

Figure 22, Beamforming with four-column antenna

		Optimum application	Downlink (TM)
Single-column	45° HBW	Dense site spacing, high traffic areas	MIMO (2 and 3 optimal; 4 and 6 possible)
	65° HBW	All sites, all speeds. Best all-around	
	85° HBW	Rural sites, coverage challenges	
Two-column	0.7λ column spacing	Correlated/beamforming; cell edge DL throughput	MIMO, BF (2, 3, 4, 5 and 6)
	1λ column spacing	Decorrelated/multi-layer; DL cell peak throughput; UL cell edge throughput	MIMO (2 and 3 optimal; 4 and 6 possible)
Four-column	0.5λ column spacing	Correlated/beamforming; DL cell edge throughput	BF, MIMO (8 optimal; 3, 4, 5, 6, 7 and 9 possible)
	0.65λ column spacing	Best column pattern/uplink cell edge throughput	BF, MIMO (8 and 9 optimal; 3, 4, 5, 6 and 7 possible)

Table 5, Antenna selection

Multiple-cell beamforming

In locations lacking a dominant serving cell, it is preferable to mitigate intercell interference using coordinated transmission. Coordinated beamforming across multiple cells has led to a new transmission mode known as multiple-cell beamforming (MC-BF). The concept has been studied in 3GPP as coordinated multipoint (CoMP) transmission/reception. First standardized in LTE 3GPP Rel. 11 as TM10 (see Table 4, LTE transmission), it is also sometimes referred to as network MIMO, distributed MIMO, multiple-cell MIMO, etc.[ii]

The idea is to have jointly designed beamforming weights from multiple cells, such that the contributing cells transmit their signals toward users constructively. MC-BF can be classified as **joint** or **coordinated**. In joint MC-BF, two or more cells jointly and constructively transmit signals to a single UE using the same time-frequency resources. Coordinated MC-BF coordinates scheduling and beamforming across different cells so they are aligned to reduce interference.[ii]

Figure 22 shows simulation results for spectral efficiency improvements with coordinated MC-BF compared to 2x2 MIMO.

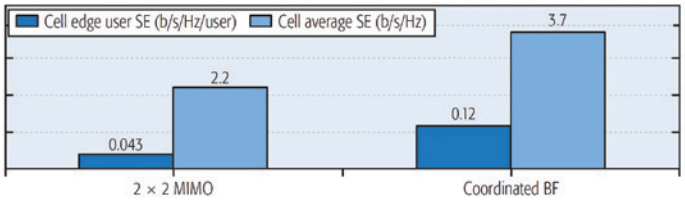

Figure 23, Downlink performance of multiple-cell beamforming[ii]

Massive MIMO beamforming

Massive MIMO has recently gained the industry's attention as one of the key technologies for achieving 5G performance targets. The initial version of a massive beamforming scheme in 3GPP—that is, full-dimension MIMO (FDMIMO)—is being standardized in Release 13[ii].

The technology involves the use of a large excess of service antennas over active terminals. When arranged in large arrays, massive MIMO allows narrower, focused and highly directed beams. This improves spectral and energy efficiencies, leading to higher capacities.

Figure 24, The Lund University massive MIMO testbed (LuMaMi)

As massive MIMO relies on spatial multiplexing and precoding, the base station needs sufficient knowledge of the uplink and downlink channels. For uplink information, terminals can simply send pilot signals—based on which the base station estimates the channel responses to each of its terminals.

Acquiring downlink channel conditions, however, is more challenging. LTE standards require the base station transmit pilot waveforms that the terminals can use to estimate channel status information (CSI). The CSI is quantized and relayed back to the base station as CQI, PMI and RI information. The number of pilot waveforms and channel responses each terminal must estimate is proportional to the number of antennas[xiv]. This eventually adds tremendous computational overheads, considering the massive MIMO antenna numbers.

Using LTE-TDD, versus FDD, and channel reciprocity, DL channel conditions can be estimated with far less complexity. As a result, TDD may be a more promising candidate for 5G systems with large-scale antenna arrays. It should be noted that massive MIMO with LTE-FDD is also possible, but comes with higher complexity and cost.

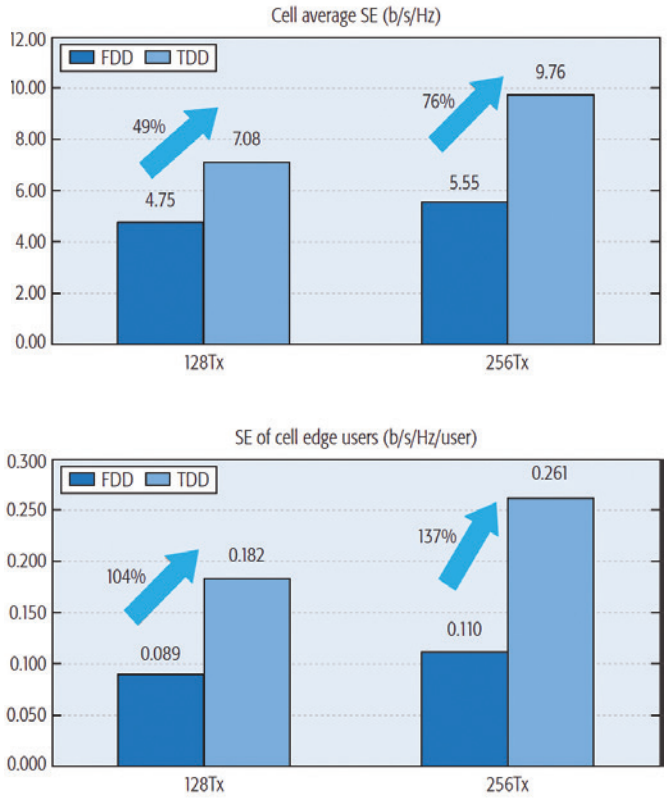

Figure 25, Spectral efficiency simulation for massive beamforming FDD versus TDD[ii].

Conclusion

Smart antennas usually refer to adaptive beamforming antennas. The technology requires two-dimensional (planar) arrays of radiating elements, and connected radios with signal processing techniques that enable steering the beams and nulls in vertical and horizontal domains.

Using transmission modes 8, 9 and 10, LTE supports classical beamforming. It can also enable another implicit beamforming effect by taking advantage of channel precoding.

Today, 2x2 MIMO LTE-TDD horizontal beamforming can be realized using external radios attached to four cross-polarized antenna columns (eight ports). The configuration can also support multi-user MIMO operation.

In the future, massive and full dimension MIMO—using excessive transmitters and radiating antenna elements arranged in massive arrays—will allow narrower, focused and highly directed beams. This will dramatically improve the spectral and energy efficiencies needed in tomorrow's 5G systems.

References

[i] Chuck Powell, Technical Analysis: Beamforming vs. MIMO Antennas, June 2014.

[ii] Shanzhi Chen, Shaohui Sun, Qiubin Gao, and Xin Su, Adaptive Beamforming in TDD-Based Mobile Communication Systems: State of the Art and 5G Research Directions, IEEE Wireless Communications, December 2016.

[iii] Mohamed Nadder, Antenna myths for base station antennas, CommScope white paper, January 2016.

[iv] Robert J. Mailloux, Phased Array Antenna Handbook, second edition, Artech House.

[v] Butler, J., and R. Lowe, "Beamforming Matrix Simplifies Design of Electronically Scanned Antennas," Elect. Design, Vol. 9, April 12, 1961, pp. 170–173.

[vi] Theodore C. Cheston, Radar Handbook, Chapter 7, McGraw Hill, 1990.

[vii] Randall T. Becker, Agilent Technologies, Precoding and Spatially Multiplexed MIMO in 3GPP Long-Term Evolution, High Frequency Electronics.

[viii] 4G Americas, MIMO and smart antennas for mobile broadband systems, June 2013.

[ix] http://rfmw.em.keysight.com/wireless/helpfiles/89600B/webhelp/subsystems/lte/content/lte_antenna_paths_ports_explanation.htm

[x] Rohde and Schwarz, Continuing in the direction of LTE-Advanced: the latest test signals for LTE Rel. 9.

[xi] 3GPP TS 36.213 V13.1.1, Physical layer procedures.

[xii] Kevin Linehan and Julius Robson, White paper: "What base station antenna configuration is best for LTE-Advanced?"

[xiii] Ivy Y. Kelly, Martin Zimmerman, Ray Butler and Yi Zheng, Base station antenna selection for LTE networks, CommScope white paper, May 2015.

[xiv] Erik G. Larsson, ISY, Linköping University Sweden. Ove Edfors and Fredrik Tufvesson, Lund University, Sweden. Thomas L. Marzetta, Bell Labs, Alcatel-Lucent, United States, Massive MIMO for Next Generation Wireless Systems, IEEE Communications Magazine, February 2014.

CommScope pushes the boundaries of communications technology with game-changing ideas and ground-breaking discoveries that spark profound human achievement.
We collaborate with our customers and partners to design, create and build the world's most advanced networks. It is our passion and commitment to identify the next opportunity and realize a better tomorrow. Discover more at commscope.com

COMMSCOPE®

commscope.com

Visit our website or contact your local CommScope representative for more information.

WP-1114971-EN (09/18)